An Accurate Diffraction Ultrasound Tomography Images Reconstruction Algorithm Based on LS_NUFFT

Jie Fang Ping Yu
College of Mechanical and Electronic Engineering,
West Anhui University,
Liu'an, Anhui 237012, China
Email: 63640193@qq.com

Zhiyuan Weng Min Kong
Intelligent Lighting and Display Technology Engineering
Center, West Anhui University
Liu'an, Anhui 237012, China

Abstract: According to the Fourier diffraction projection theory, the Fourier transform of projection data from multi-band frequency ultrasonic is distributed over complex plane in form of different radius arcs. The classical filtered back projection（FBP）algorithm isn't fit for distributing of the *k* space data, and the conventional gridding data interpolation on non-Cartesian data would produce much artifact . The least squares nonuniform fast Fourier transform(LS_NUFFT) is brought forth by Liu and Nguyen and applied in MRI image reconstruction. The LS_NUFFT is apply successfully in diffraction ultrasound tomography image reconstruction for the first time and the best kernel matrix size is proved by experiment. The reconstruction experiments based on LS_NUFFT, Min-max NUFFT and GFFT algorithms are done respectively, the reconstruction quality of LS_NUFFT is much better than Min-max method and GFFT method .

Keywords: diffraction tomography; Fourier diffraction projection theory; LS_NUFFT;GFFT

I. INTRODUCTION

Ultrasound tomography with diffracting sources is an important type of acoustic imaging. Since the used wavelengths are comparable to the object feature dimensions, wave phenomena such as diffraction become significant. Consequently, the straight ray tomography theory is no longer applicable. The analog of the Fourier Slice Theorem used in straight ray tomography is the Fourier Diffraction Theorem. Using this theorem, image reconstruction in diffraction tomography can be considered as a problem of signal reconstruction from nonuniform frequency samples. Conventional gridding methods have used predefined gridding kernel functions, such as triangle, Gaussian, *sinc*, and Kaiser-Bessel functions, and so forth. The NUFFTs calculate optimal kernels with selected scaling function to minimize the interpolation error[1-4]. In the gridding algorithm, the inverse Fourier transform is estimated by convolving the density compensated data with a finite kernel, sampling onto a Cartesian grid, performing an FFT and multiplying by an apodization correction function, and the interpolation on non - Cartesian data would produce much artifact . To overcome the shortage of conventional gridding method in diffraction ultrasound tomography reconstruction, an accurate reconstruction algorithm is proposed in this paper using nonuniform FFT (NUFFT). The cosine scaling factor of least square nonuniform FFT(LS_NUFFT) used for the reconstruction enables closed form solution for the kernel matrix and get different size matrix with it; then the non-Cartesian sampling projection data is interpolated to Cartesian grid using this kernel matrix with optimal size;finally image reconstruction is fulfilled by 2-dimensional FFT. Reconstruction results thus obtained compared with the other two NUFFT methods reduce to a large extent the reconstruction error based on its norm 2.

II. PRINCIPLES OF DIFFRACTION TOMOGRAPHY

Given a projection $u_\theta(\vec{r})$ of the forward scattered field $u_s(\vec{r})$ obtained by illuminating an object $O(x,y)$ with a plane wave, the following equation holds[5-6]:

$$FT\{u_\theta(r)\}(k) = FT\{O(x,y)\}\{k_{xp}, k_{yp}\} \qquad (1)$$

where

$$k_{xp} = k\cos\theta - (\sqrt{k_0^2 - k^2} - k_0^2)\sin\theta \qquad (2)$$

$$k_{yp} = k\sin\theta + (\sqrt{k_0^2 - k^2} - k_0^2)\cos\theta) \qquad (3)$$

In other words, the Fourier transform of the projection gives the values of the 2-D Fourier transform of the object along a semicircular arc in the spatial frequency domain, as depicted in Fig. 2. The transform corresponds to upper Ewald semicircle when operating in transmission mode , while the lower Ewald semicircle refers to reflection mode. Since wave phenomena obey the superposition principle, illuminating the object with a wave consisting of a set of frequencies (referred to as *broad-band illumination*), rather than a monochromatic wave, will produce samples along a set of semicircular arcs with different radii. Hence, a single projection potentially

contains much more information about the object than a single projection in straight ray tomography. By taking advantage of this fact, one can achieve sufficient image quality with fewer projections[7].

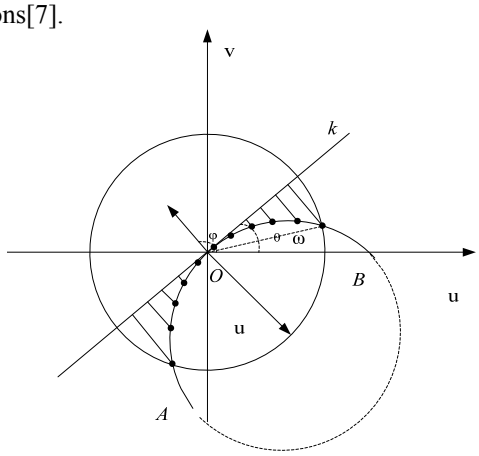

Figure 1.Acquisition of a single diffraction projection is related to the k-space sampling along a semi-circular arc

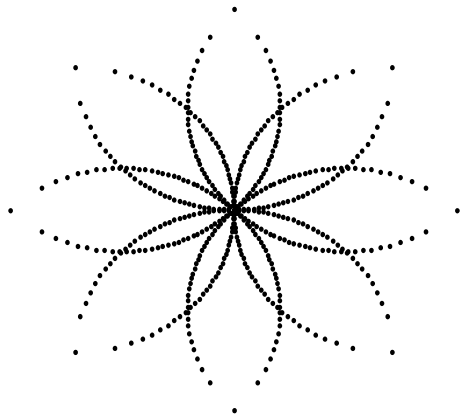

Figuer2. Distribution of the data according Fourier diffraction projection Theorem. in frequency domain

III.RECONSTRUCTION

The final diffraction ultrasound tomography form of the direct summation reconstruction is:

$$I(m,n)=\sum_{p=1}^{M} s_p C_p \exp(i2\pi(xk_{mp}+yk_{np})) \qquad (4)$$

The computation complexity direct summation reconstruction approach is about O(N^4), N represents the number of pixels in reconstructed image.the amout of computation is too large.

The final diffraction ultrasound tomography form of LS_NUFFT reconstruction is[8]:

$$I(m,n)=(s_c(m)s_c(n))^{-1}\times \sum_{k1=-\mu N/2}^{\mu N/2-1}\sum_{k2=-\mu N/2}^{\mu N/2-1}\tau_{k1,k2}\exp(i2\pi(mk1+nk2)/\mu) \qquad (5)$$

Where

$$\tau_{k1,k2}=\sum_{[\mu k_{xp}]+j1=k1}\sum_{[\mu k_{yp}]+j2=k2} s_p C_p \rho_1(j1,k_{mp})\rho_2(j2,k_{np}) \qquad (6)$$

The computation complexity to obtain $\rho 1$, and $\rho 2$ in Eq.(6)is O(q^2M) . and the complexity for the 2D IFFT step in Eq. (5) is O($(mN)^2\log^2(mN)$) . The total complexity is then O($(mN)^2$log2(mN)+q^2M).the amout of computation, Amount of computation using LS-NUFFT is much smaller than the direct summation method.

In summary, the LS_NUFFT algorithm consists of the following six steps:

1. According to the Fourier diffraction projection theory, gaining projection data s_p and its coordinate k_{xp}, k_{yp}.
2. Generate the kernel matrices $\rho 1$, $\rho 2$ corresponding to k_{mp}, k_{np} and the scale factor s_c.
3. Density compensation by Voronoi diagrams[9,10].
4. Obtain convolution $\tau_{k1,k2}$ of $s_p C_p$ and the kernel matrixes $\rho 1$, $\rho 2$.
5. Perform 2D IFFT on $\tau_{k1,k2}$.
6. Re-scale the result by $(s_c(m)s_c(n))^{-1}$.

IV. CHOOSING A LS_NUFFT KERNEL

We may choose two different accuracy factors, namely (1) the Gaussian $s_j=e^{-b(\frac{2\pi j}{\mu N})}$ and (2) the cosine $s_j=\cos\frac{\pi j}{Nm}$ accuracy factors. In particular, the cosine scaling factor used in Liu and Nguyen's report is adopted in this paper for the LS_NUFFT, which enables closed form solution for the kernel function[11].

$$\rho_{j,c_p}=\mathbf{G}_{j,k}a_{k,c_p}, \qquad j,k=-\frac{q}{2}\cdots\frac{q}{2}, p=1,\cdots,M \qquad (7)$$

where

$$\mathbf{G}=\mathbf{F}^{-1},\mathbf{F}_{j,k}=\begin{cases} N & j=k \\ \dfrac{-2i\sin(\pi(j-k)/\mu)}{1-\exp(i2\pi(j-k)/\mu N)} & j\neq k \end{cases} \qquad (8)$$

$$a_{k,c_p}=i\sum_{\gamma=-1,1}\frac{\sin[\frac{\pi}{2\mu}(2k-\gamma-2\{\mu c_p\}]}{1-\exp(i\frac{\pi}{N\mu}(2\{\mu c_p\}-2k+\gamma))} \qquad (9)$$

$$\{\mu c_p\}=\mu c_p-[\mu c_p]$$

where μ is the oversampling factor and q is the kernel size.The kernel varies from sample to sample, but it is only

dependent on the location of each sample.

V.SIMULATION

In order to avoid forward-projection errors, we used an analytic Shepp-Logan phantom. This phantom is a superposition of ellipses representing features of the human brain (see Figure 3.1). The advantage of such phantom is that its Fourier transform has a simple analytical expression. The continuous Cartesian 2D Fourier transform of an ellipse of intensity ρ, semi-axes of length A and B , and orientation angle α , is given (up to a multiplicative constant) by

$$E_i(u,v)=\rho e^{-i(ux_0+vy_0)}\times \frac{AJ_1\{B[((u\cos a+v\sin a)A/B)^2+(-u\sin a+v\cos a)^2]^{\frac{1}{2}}\}}{[((u\cos a+v\sin a)A/B)^2+(-u\sin a+v\cos a)^2]^{\frac{1}{2}}} \quad (10)$$

$$E(u,v)=\sum_{i=0}^{N}E_i(u,v) \quad (11)$$

Sinograms were created by appropriate sampling of $E(u,v)$ in accordance with the Fourier Slice Theorem where J_1 is the first-order Bessel function of the first kind, and the Fourier transform of the whole phantom is given by (radon transform case) and the Fourier diffraction theorem (diffraction case).

To evaluate the reconstruction results, we used a measure of minimum distance between the images under test and the image reconstructed using direct summation approach.

$$ERROR_2=\left\|\mathbf{I}_{recon}-\mathbf{I}\right\|_2 \Big/ \left\|\mathbf{I}\right\|_2 \quad (12)$$

$ERROR_2$is image reconstruction error based on $\ell 2$ norm, $\mathbf{I}$ and $\mathbf{I}_{recon}$ are original image and reconstruction image with NUFFT method respectively.

A. Selecting μ of LS_NUFFT kernel

The size of kernel matrix is $(\mu+1)\times M$,The“64×64 Shepp-Logan phantom” is utilized here for computer simulation study，the number of data sample point is 2×8192, then we chose the best μ for the reconstruction.

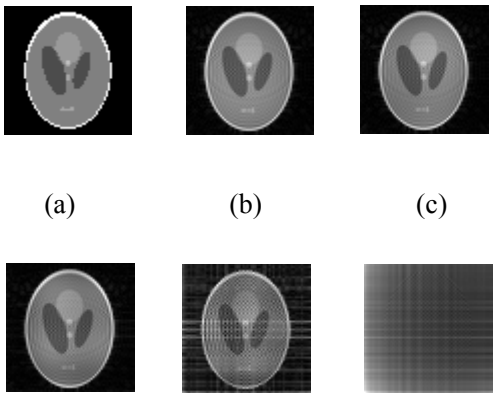

(a) (b) (c)

(d) (e) (f)

Figure3. (a) 64×64“Shepp and Logan”，(b)、(c)、(d)、(e)、(f),The reconstruction images of LS_NUFFT method with m=2,q=2,4,6,8,10 respectively.

Table1:THE COMPARISON OF RECONSTRUCTION ERROR OF LS_NUFFT METHOD WITH DIFFERENT q

q=	$ERROR_2$	Total time/s
2	0.2316	7.42
4	0.2291	8.95
6	0.2379	10.62
8	0.4446	13.41
10	0.9708	17.61

Figure .3 and Table 1 shows the best reconstruction results is gained at q=4, and the results become much bad at q=8,10 , so the next experiments we select μ =2 and q=4.

B.Comparing of three reconstruction methods

In this section, the GFFT and Min-max NUFFT[12] gridding is formulated the same way for comparison,let μ =2,q=8 (q≥4bπ) in GFFT and μ =2,q=4 in LS_NUFFT. Figure 4 is an original image, b,c,d are reconstructed image from GFFT,Min-max NUFFT and LS_NUFFT method respectivly.

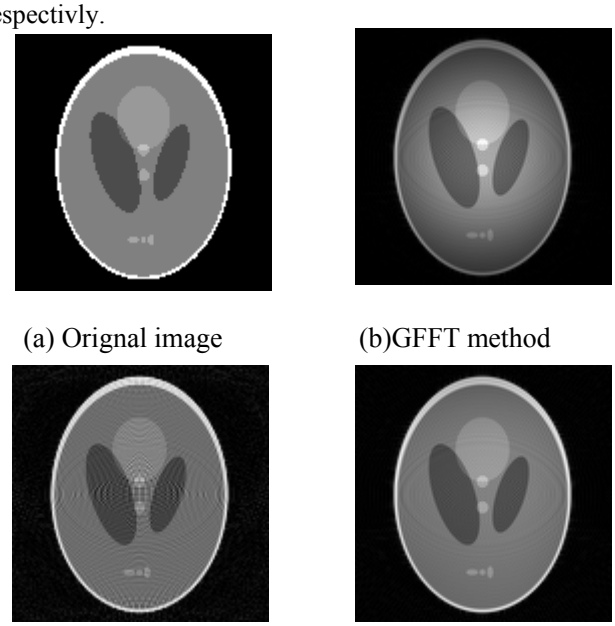

(a) Orignal image (b)GFFT method

(c)Min-Max method (d)LS method

Figure.4 128×128 Shepp and Logan original image and reconstruction images of three method under 16384 projection data.

TABLE2 THE RECONSTRUCTION ERROR AND TIME OF 128×128 “ SHEPP AND LOGAN” OF THREE DIFFIRENT METHOD

Image(128^2)	GFFT	Min-Max	LS_NUFFT
Sample points	1×16384	1×16384	1×16384
$ERROR_2$	0.3346	0.2744	0.2291
Total time(s)	90.980	33.88	40.99

Table 2 illustrates the performance comparisons using digital phantom data, it shows that the $ERROR_2$ of the LS_NUFFT image to is smaller than GFFT and Min-Max method , and the Min-max NUFFT method costs the least reconstruction time of all.As can be seen from the figure.4(b) , image region of phantom using GFFT reconstruction method is dark, it can be seen from figurer.4(c), Gibbs phenomenon in Min-max method reconstructed phantom image region is much serious. By b, c, d of figure.4, we can see the reconstruction of LS_NUFFT works best.

VI.CONCLUSION

The final renconstructive image is a convolution of the point spread function and acoustic field distribution, thus the error of image is proportional to the energy of convolution region, and the error in high energy region leak to the energy region around it.LS_NUFFT method compared with GFFT, Min-max method, the kernels on the interpolation accuracy is improved to a large extent, so we can see the gibbs phenomenon using LS_NUFFT method is more slightly than GFFT and Min-max method, although th phenomenon does not completely eliminate. thereby reducing the point spread function leads to less sharp image intensity of leakage . In addition, the matrix of convolution kernel is relatively small, its reconstruction speed is faster than GFFT method.

VII.ACKNOWLEDGMENT

This work is supported by NFSC(61302179, 61303209), and key science foundation for outstanding yong talent of Anhui (2013SQRL072ZD),and Anhui provincial natural science foundation(1408085MA20, 1301023004), and the natural science research project of West Anhui University (0041014006).

REFERENCES

[1] Arfanakis K, Tamhane A A, Pipe J G, et al. k-space under sampling in PROPELLER imaging. Magnetic Resonance in Medicine, 2005, 53(3): 675-683.

[2] Feng yanqiu, Chen wufan,Yan Gang, et al. A new algorithm for sampling density compensation in the gridding of PROPELLER MRI data. Acta Electronica Sinica, 2007, 35(4): 766-768.

[3] Du Q, Wang D S. Recent progress in robust and quality Delaunay mesh generation. Journal of Computational and Applied Mathematics, 2006, 195(1/2): 8-23.

[4] Jung Kuk Kim, J A Fessler, Zhengya Zhang. Forward-projection architecture for fast iterative image reconstruction in X-ray CT. IEEE Transactions on Signal Processing, 2012, 60(10): 5508-5518.

[5] Zhang D W, Tao J X. A novel gridding algorithm using NUFFT with applications to ultrasound diffraction tomography . Proceedings of the 2nd International Conference on Bioinformatics and Biomedical Engineering. Shanghai, China: IEEE, 2008. 2473-2476.

[6] Fang Jie, Wei Sui, Su Shoubao. The multi-band diffraction ultrasound tomography images based on the total variation denoised algorithm. Acta Electronica Sinica, 2009, 28(4): 828-832.

[7] Bronstein M M, Alexander M. B, Azhari.H Reconstruction in diffraction ultrasound tomography using non-uniform FFT . IEEE transaction on medical imaging 2002,21(11):1395-1401

[8] Liewei Sha,Hua Guo,and Allen W. Song An improved gridding method for spiral MRI using nonuniformfast Fourier transform

[9] Fangjie, Liu renjin.Study on Image Reconstruction of Diffraction Tomography With Density Compensation Algorithm by Voronoi Diagrams. Acta Electronica Sinica, 2014, 42(7): 1268-1272.

[10] Zhou heqin, Tan pei, Hou Chenggong. A Voronoi diagram-based algorithm for the gridding of PROPELLER MRI data. Journal of University of Science and Technology of China, 2008, 38(7): 783-786.

[11] Dutt A, Rokhlin V. Fast Fourier transforms for nonequispaced data, II. Applied and Computational Harmonic Analysis, 1995, 2(1): 85-100.

[12] Fessler J A, Sutton B P. Nonuniform fast Fourier transforms using min-max interpolation. IEEE transactions on Signal Processing, 2003,51 (2):560–574 ,21(11):1395-1401